Rate processes in a delayed, stochastically driven, and overdamped system

Steve Guillouzic, Ivan L'Heureux, and André Longtin
Ottawa-Carleton Institute for Physics, University of Ottawa, Ottawa, Ontario, Canada K1N 6N5
(Received 16 November 1999)

A Fokker-Planck formulation of systems described by stochastic delay differential equations has been recently proposed. A separation of time scales approximation allowing this Fokker-Planck equation to be simplified in the case of multistable systems is hereby introduced, and applied to a system consisting of a particle coupled to a delayed quartic potential. In that approximation, population numbers in each well obey a phenomenological rate law. The corresponding transition rate is expressed in terms of the noise variance and the steady-state probability density. The same type of expression is also obtained for the mean first passage time from a given point to another one. The steady-state probability density appearing in these formulas is determined both from simulations and from a small delay expansion. The results support the validity of the separation of time scales approximation. However, the results obtained using a numerically determined steady-state probability are more accurate than those obtained using the small delay expansion, thereby stressing the high sensitivity of the transition rate and mean first passage time to the shape of the steady-state probability density. Simulation results also indicate that the transition rate and the mean first passage time both follow Arrhenius' law when the noise variance is small, even if the delay is large. Finally, deterministic unbounded solutions are found to coexist with the bounded ones. In the presence of noise, the transition rate from bounded to unbounded solutions increases with the delay.

PACS number(s): 02.50.Ey, 02.30.Ks, 05.40.−a

I. INTRODUCTION

When considering noise-driven multistable systems, it is often of interest to characterize the noise-induced rate processes between basins of attraction. Much work has been devoted to this issue for nondelayed stochastic differential equations, whether they be driven by white noise [1–4], Ornstein-Uhlenbeck noise [5,6], or colored dichotomous noise [7–12]. In general, however, the analytical tools used to study nondelayed stochastic differential equations are not directly applicable to the characterization of stochastic delay differential equations (SDDE's) because of the non-Markovian character of these equations. This is unfortunate since SDDE's play an increasingly important role in several fields of research. For instance, SDDE's are used in both physiology [13–16] and optics [17,18] to model noise-driven systems exhibiting delayed feedback. Furthermore, noise-induced rate processes in delayed sytems are of current interest. Indeed, rate processes in noise-driven inertial systems damped according to a memory kernel were recently investigated [19–21]. Such a memory kernel is formally equivalent to a distribution of time delays. Noise-induced rate processes are also being studied in the context of delayed maps [22] and integrate-and-fire models [23]. In addition, a system of noise-driven delayed coupled differential equations was the subject of a recent study [24].

In the case of SDDE's, a univariate Fokker-Planck formulation was recently proposed [25]. Even though the resulting Fokker-Planck equation (FPE) cannot in general be solved exactly, approximation schemes may be used. One such scheme, based on a separation of time scales and applicable to multistable systems, is presented in this paper. This method leads to a simplified FPE that can be used in conjunction with standard techniques developed for Markovian systems. One such technique, elaborated by Wu and Kapral [2], allows the rates appearing in a phenomenological noise-induced rate law to be expressed solely in terms of the steady-state probability density and the noise variance when the latter is small. Another standard technique [26] allows the same to be accomplished for the mean first passage time (MFPT), which is the mean time required to reach a given point in space for the first time when starting from another given point. In this case, however, the result is applicable whether the noise variance is small or large.

Using the separation of time scales approximation, both of these techniques are applied in this paper to study the stochastic evolution of a particle in a delayed symmetric quartic potential. This system has been chosen since it is the archetypical example of symmetric bistable potentials, which are used in a variety of applications [27], and can help capture several essential characteristics of delayed multistable systems. Furthermore, delayed-coupled oscillator systems have been the subject of recent work [24,28–31]. Studying the role of delays in an isolated multistable system can lead to a better understanding of their importance in coupled multistable systems. Delayed dynamics often occur naturally in this context because of the finite speed at which information is transmitted between elements.

The steady-state probability density appearing in formulas of the transition rates and the MFPT may be determined from simulations or using an approximation scheme, such as the recently proposed small delay expansion technique [25]. In this paper, the transition rates and MFPT's obtained using a steady-state probability density determined from simulations or from the small delay expansion are compared with the values obtained directly from simulations.

The Fokker-Planck formulation of SDDE's is summarized in Sec II. Section III then introduces the separation of time scales assumption, and Sec. IV reviews the small delay approximation. These concepts are applied to the delayed

quartic potential in Sec. V. Finally, concluding remarks are given in Sec. VI.

II. STEADY-STATE PROBABILITY DENSITY

We consider the overdamped motion of a particle evolving in a delayed and stochastically driven double-well potential $V(x_o)$, with the separatrix located at $x_o=0$. The time evolution of such a system over the whole real axis is given by the stochastic delay differential equation

$$dx(t)=f(x(t-\tau))dt+\sigma dW(t), \tag{1}$$

where x is the state variable, τ is the delay, σ scales the noise amplitude, and

$$f(x_o)\equiv-\frac{d}{dx_o}V(x_o) \tag{2}$$

describes the deterministic evolution. In this paper, x_o and x_τ are used as dummy variables, and do not necessarily refer to $x(t)$ and $x(t-\tau)$, nor to initial conditions. The quantity $W(t)$ appearing in Eq. (1) is a Wiener process whose initial condition is 0 at time $t=0$ and is hence characterized by $\langle W(t)\rangle=0$ and $\langle W^2(t)\rangle=t$, where $\langle\cdots\rangle$ denotes an ensemble average (average over realizations). Since Eq. (1) involves delayed dynamics, its integration forward in time for $t>t'$ requires the initial condition $\{x'(t)|t\in[t'-\tau,t']\}$.

Let $p(x_o,t_o;x_\tau,t_\tau|x',t')dx_o dx_\tau$ be the probability that $x(t_o)\in[x_o,x_o+dx_o]$ and $x(t_\tau)\in[x_\tau,x_\tau+dx_\tau]$, given that $x(t)=x'(t)$ for all $t\in[t'-\tau,t']$. Thus $p(x_o,t_o;x_\tau,t_\tau|x',t')$ is a bivariate probability density that is conditional only on the initial condition $\{x'(t)|t\in[t'-\tau,t']\}$. The univariate probability density $p(x_o,t_o|x',t')$ can then be defined as

$$p(x_o,t_o|x',t')\equiv\int_{-\infty}^{\infty}dx_\tau p(x_o,t_o;x_\tau,t_\tau|x',t'). \tag{3}$$

It has been shown [25] that the evolution of this univariate probability density is given by the well-known Fokker-Planck equation

$$\frac{\partial}{\partial t}p(x_o,t|x',t')=-\frac{\partial}{\partial x_o}\{\overline{f}(x_o,t|x',t')p(x_o,t|x',t')\}+\frac{\sigma^2}{2}\frac{\partial^2}{\partial x_o^2}p(x_o,t|x',t'), \tag{4}$$

where

$$\overline{f}(x_o,t_o|x',t')\equiv\int_{-\infty}^{\infty}dx_\tau f(x_\tau)\frac{p(x_o,t_o;x_\tau,t_o-\tau|x',t')}{p(x_o,t_o|x',t')} \tag{5}$$

is called the conditional average drift (CAD) and is the average of dx/dt evaluated at time t_o given that $x(t_o)=x_o$. As the delay vanishes, $\overline{f}(x_o,t_o|x',t')$ tends to $f(x_o)$ and Eq. (4) approaches the usual FPE associated with a nondelayed stochastic differential equation (SDE).

Assuming the existence of the steady-state limits

$$\overline{f}^s(x_o)\equiv\lim_{t_o\to\infty}\overline{f}(x_o,t_o|x',t')$$

and

$$p^s(x_o)\equiv\lim_{t_o\to\infty}p(x_o,t_o|x',t'),$$

reflecting boundary conditions lead to the so-called potential solution

$$p^s(x_o)=N\exp\left(\frac{2}{\sigma^2}\int_c^{x_o}dy\,\overline{f}^s(y)\right), \tag{6}$$

where c is arbitrary. The constant N is determined from the normalization condition

$$\int_{-\infty}^{\infty}dx_o p^s(x_o)=1$$

and implicitly depends on τ.

III. NOISE-INDUCED RATE PROCESSES

A. Separation of time scales approximation

Equations (4) and (5) constitute together a generally nontrivial integrodifferential equation. However, if the CAD $\overline{f}(x_o,t_o|x',t')$ is successfully determined by other means, Eq. (4) may then be solved independently from Eq. (5). In this line of thought, when considering noise-induced processes in the double-well potential $V(x_o)$, the CAD $\overline{f}(x_o,t_o|x',t')$ can in certain circumstances be approximated by its steady-state limit, which may be easier to evaluate. For instance, let τ_{pop} be the time scale over which $p(x_o,t_o;x_\tau,t_o-\tau|x',t')$ equilibrates between the four quadrants of the $x_o x_\tau$ plane, and τ_{int}, the time scale over which this bivariate probability density relaxes within each of the two quadrants for which x_o and x_τ are of the same sign. If τ_{pop} is much larger than the delay τ, the probability that the particle undergoes a transition from one well to the other within τ units of time must be very small. Therefore $p(x_o,t_o;x_\tau,t_o-\tau|x',t')$ must be much smaller when x_o and x_τ are of opposite sign than when they are of the same sign. The CAD $\overline{f}(x_o,t_o|x',t')$, defined by Eq. (5), can in this case be approximated by

$$\overline{f}(x_o,t_o|x',t')\simeq\int_{-\infty}^{0}dx_\tau f(x_\tau)\frac{p(x_o,t_o;x_\tau,t_o-\tau|x',t')}{p(x_o,t_o|x',t')} \tag{7}$$

when $x_o<0$, and by

$$\overline{f}(x_o,t_o|x',t')\simeq\int_{0}^{\infty}dx_\tau f(x_\tau)\frac{p(x_o,t_o;x_\tau,t_o-\tau|x',t')}{p(x_o,t_o|x',t')} \tag{8}$$

when $x_o>0$. Furthermore, in each of the two quadrants for which x_o and x_τ are of the same sign, the bivariate probability density $p(x_o,t_o;x_\tau,t_o-\tau|x',t')$ is approximately proportional to its steady-state limit for all times much larger than τ_{int}. Since $p(x_o,t_o;x_\tau,t_o-\tau|x',t')$ is much larger in

these two quadrants than in the other two quadrants when $\tau_{pop} \gg \tau$, the univariate probability density $p(x_o,t_o|x',t')$ defined by Eq. (3) is then approximately proportional to its steady-state limit separately in each of the two wells and the ratio $p(x_o,t_o;x_\tau,t_0-\tau|x',t')/p(x_o,t_o|x',t')$ is approximately equal to its steady-state limit. In this regime, Eqs. (7) and (8) lead to

$$\overline{f}(x_o,t_o|x',t') \simeq \overline{f^s}(x_o). \tag{9}$$

The CAD $\overline{f}(x_o,t_o|x',t')$ can thus be approximated by its steady-state limit for times much larger than τ_{int} when $\tau_{pop} \gg \tau$. If furthermore $\tau_{pop} \gg \tau_{int}$, the approximate FPE

$$\frac{\partial}{\partial t}p(x_o,t|x',t') = -\frac{\partial}{\partial x_o}\{\overline{f^s}(x_o)p(x_o,t|x',t')\} + \frac{\sigma^2}{2}\frac{\partial^2}{\partial x_o^2}p(x_o,t|x',t') \tag{10}$$

can be used to study the equilibration of the probability density $p(x_o,t_o|x',t')$ between the two wells of the bistable potential $V(x_o)$. It is interesting to note that the steady-state CAD $\overline{f^s}(x_o)$ is fully determined by the steady-state probability density $p^s(x_o)$ through Eq. (6).

B. Phenomenological transition rate

When dealing with experimental measurements, it is often of interest to consider the average evolution of an ensemble of systems. In order to do so, population numbers for both wells are defined as

$$N_A(t_o|x',t') \equiv \int_{-\infty}^{0} dx_o p(x_o,t_o|x',t') \tag{11}$$

and

$$N_B(t_o|x',t') \equiv \int_{0}^{\infty} dx_o p(x_o,t_o|x',t'). \tag{12}$$

Clearly, $N_A(t_o|x',t')+N_B(t_o|x',t')=1$. When $\tau_{pop} \gg \tau_{int}$, projection operator techniques applied on Eq. (10) lead to the phenomenological equation [2]

$$\frac{d}{dt}N_A(t|x',t') = -k_f N_A(t|x',t') + k_r N_B(t|x',t'), \tag{13}$$

where k_f and k_r are phenomenological rate constants.

For a small noise variance σ^2 and a potential $V(x_o)$ symmetrical with respect to its local maximum at $x_o=0$, the rate constants are approximately given by [2]

$$k \equiv k_f = k_r = \frac{\sigma^2}{4}\left[\int_0^\infty dx p^s(x) \times \int_0^x \frac{dy}{p^s(y)}\left(1-2\int_0^y dz p^s(z)\right)\right]^{-1}. \tag{14}$$

Furthermore, in this case, both population numbers asymptotically approach 1/2 with time, and Eq. (13) leads to

$$N_A(t|x',t') = \frac{1}{2} + \left(N_A(t'|x',t') - \frac{1}{2}\right)\exp(-(t-t')/\tau_{pop}), \tag{15}$$

where

$$\tau_{pop} = \frac{1}{2k} \tag{16}$$

is the time scale over which the population numbers $N_A(t_o|x',t')$ and $N_B(t_o|x',t')$ relax to their steady-state limits.

C. Mean first passage time

For a system described by an autonomous FPE like Eq. (10), the mean first passage time $T(x_1,x_2)$ required to reach $x=x_2$ from $x=x_1$ can be determined through the use of the backward Fokker-Planck equation [26]. This method leads to

$$T(x_1,x_2) = \frac{2}{\sigma^2}\int_{x_1}^{x_2}\frac{dy}{p^s(y)}\int_{-\infty}^{y} dz p^s(z) \tag{17a}$$

when $x_1 < x_2$, and to

$$T(x_1,x_2) = \frac{2}{\sigma^2}\int_{x_2}^{x_1}\frac{dy}{p^s(y)}\int_{y}^{\infty} dz p^s(z) \tag{17b}$$

when $x_1 > x_2$.

As shown by Eqs. (14) and (17), the time evolution of the system described by the SDDE (1) over time scales comparable to τ_{pop} can be easily characterized when $\tau_{pop} \gg \tau_{int}$ and $\tau_{pop} \gg \tau$ (irrespective of the relation between τ and τ_{int}), once the steady-state probability density $p^s(x_o)$ is known. To our knowledge, however, there exists no analytical or numerical method to obtain the exact solution for the steady-state probability density of a general SDDE. Thus $p^s(x_o)$ must in general be evaluated using numerical simulations or an analytical approximation such as the small delay Taylor expansion presented in the next section.

IV. EXPANSION OF THE SDDE TO $O(\tau^2)$

A quadratic expansion in powers of τ can be used to obtain an approximate nondelayed stochastic differential equation from a SDDE. This technique has already been tested on a delayed linear Langevin equation and a stochastic delayed logistic equation [25]. In both of these cases, it leads to accurate steady-state probability densities and steady-state CAD's for small values of the delay τ. Applying this $O(\tau^2)$ Taylor expansion to Eq. (1) yields the approximate SDE

$$dx = f_a(x)dt + \sigma g_a(x) dW, \tag{18}$$

where

$$f_a(x_o) \equiv f(x_o)\left(1-\tau\frac{d}{dx_o}f(x_o)\right) \tag{19}$$

and

$$g_a(x_o) \equiv 1 - \tau \frac{d}{dx_o} f(x_o). \tag{20}$$

In these equations, the subscript a stands for ''approximate.'' Carrying such a Taylor expansion to higher orders is clearly not straightforward, since there is no universally accepted way of treating terms where the noise appears with a power different than 1.

Let $p_a(x_o,t_o|x',t')dx_o$ be the probability that $x(t_o) \in [x_o, x_o + dx_o]$, given that $x(t') = x'(t')$, for a system whose evolution is given by Eq. (18). Its time evolution is given by the Fokker-Planck equation

$$\frac{\partial}{\partial t} p_a(x_o,t|x',t') = -\frac{\partial}{\partial x_o}\{f_a(x_o) p_a(x_o,t|x',t')\} + \frac{\sigma^2}{2}\frac{\partial^2}{\partial x_o^2}\{g_a^2(x_o) p_a(x_o,t|x',t')\}, \tag{21}$$

which is obtained from the approximate SDE (18). This FPE leads to the steady-state probability density

$$p_a^s(x_o) = \frac{N_a}{g_a^2(x_o)} \exp\left(\frac{2}{\sigma^2} \int_c^{x_o} dy \frac{f_a(y)}{g_a^2(y)} \right), \tag{22}$$

where N_a is the normalization constant and c is arbitrary. Equations (19), (20), and (22) can be used in conjunction with Eqs. (14), (16), and (17) to determine τ_{pop} and $T(x_1,x_2)$.

Equation (22) allows the determination of an approximate expression for the steady-state CAD $\overline{f^s}(x_o)$. Indeed, let the function $\overline{f_a^s}(x_o)$ be defined by the equation

$$p_a^s(x_o) = N_a \exp\left(\frac{2}{\sigma^2} \int_c^{x_o} dy \overline{f_a^s}(y) \right), \tag{23}$$

which corresponds to Eq. (6). Equating Eqs. (22) and (23) leads to

$$\overline{f_a^s}(x_o) = \frac{f_a(x_o) - \sigma^2 g_a(x_o) \dfrac{d}{dx_o} g_a(x_o)}{g_a^2(x_o)} = \frac{f(x_o) + \tau\sigma^2 \dfrac{d^2}{dx_o^2} f(x_o)}{1 - \tau \dfrac{d}{dx_o} f(x_o)}, \tag{24}$$

without any further approximation beyond the initial Taylor expansion. As illustrated in Ref. [25] with a system described by a stochastic delayed logistic equation, performing a further $O(\tau^2)$ Taylor expansion on Eq. (24) can reduce the range of x's over which $\overline{f_a^s}(x_o)$ is a qualitatively accurate approximation of $\overline{f^s}(x_o)$. Such an expansion must therefore be considered on a case by case basis.

V. APPLICATION TO DELAYED QUARTIC POTENTIAL

A. Deterministic evolution

The quartic potential

$$V(x_o) = \frac{\beta}{4} x^4 - \frac{\alpha}{2} x^2 \tag{25}$$

is a prototypical double-well potential. Scaling t by α^{-1} and x by $\sqrt{\alpha/\beta}$, this potential leads to the differential equation

$$dx(t) = [x(t-\tau) - x^3(t-\tau)]dt. \tag{26}$$

This delay differential equation has three fixed points: $x_1 = -1$, $x_2 = 0$ and $x_3 = 1$. Linearizing Eq. (26) around x_1 yields the equation

$$dy(t) = -2y(t-\tau)dt, \tag{27}$$

where $y(t) \equiv x(t) - x_1$. Substituting $y(t) = e^{\lambda t}$ in Eq. (27) leads to its characteristic equation

$$\lambda + 2e^{-\lambda\tau} = 0. \tag{28}$$

Using Eq. (28), all the eigenvalues λ of Eq. (27) are found to have negative real parts when $\tau < \pi/4$, therefore indicating that the fixed point x_1 is stable for these values of τ. At $\tau = \pi/4$, a pair of eigenvalues crosses the imaginary axis and the fixed point x_1 is thus unstable for $\tau > \pi/4$. By symmetry, the same analysis also applies to the fixed point x_3. On the other hand, the fixed point x_2 is always unstable, as can be seen by linearizing Eq. (26) around the origin.

The deterministic evolution of Eq. (26) can also be studied using numerical simulations. For concreteness, constant initial conditions located in the left well are considered. Furthermore, the initial conditions are chosen such as to avoid unbounded solutions (cf. Sec. V B). For small delays, up to about $\tau = 0.785$, the particle relaxes to the fixed point at $x = -1$, which is consistent with the eigenvalue analysis mentionned in the previous paragraph. For $0.786 \leqslant \tau \leqslant 1.259$, the particle oscillates periodically in the left well. As the delay reaches $\tau = 1.260$, the particle starts to cross the boundary $x = 0$ between the two wells, but does not reach the right local minimum of the potential. It is only when τ reaches 1.325 that the particle reaches both local minima in its evolution. For $1.325 \leqslant \tau \leqslant 1.522$, the trajectory is symmetrical. However, when τ reaches 1.523, the trajectory becomes asymmetrical. Around $\tau = 1.535$, the trajectory starts to undergo a series of period doubling bifurcations that culminates to an apparently chaotic solution at a value of τ between 1.538 and 1.539. As τ increases from 1.539 to 1.725, the system exhibits aperiodic behavior with interspersed periodic windows. The trajectories diverge when $\tau \geqslant 1.726$.

B. Unbounded solutions

In addition to the bistability due to the existence of two wells, another form of multistability is exhibited by Eq. (26). This is illustrated in Fig. 1. Indeed, if a sufficiently large constant initial condition over $t \in [-\tau, 0]$ is specified, the particle oscillates with an amplitude that increases indefinitely with time. This type of solution can be qualified as ''unbounded.'' In order for the system to exhibit one of the

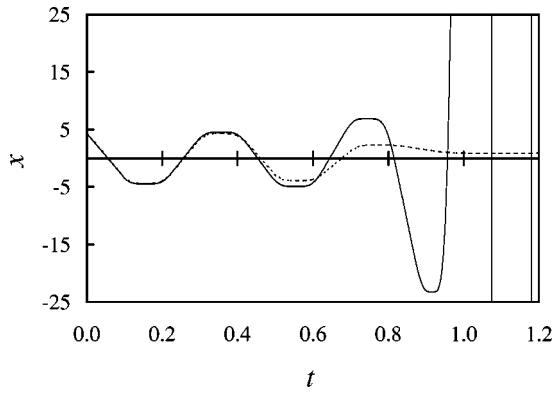

FIG. 1. Deterministic time evolution of Eq. (26) with $\tau=0.1$ for two closeby constant initial conditions. The dashed line corresponds to a constant initial condition of 4.33, from which the particle decays to a fixed point at $x=1$. The solid line, on the other hand, represents the trajectory of a particle for a constant initial condition of 4.34. In this case, the particle oscillates with an amplitude that increases with time.

asymptotic solutions described in Sec. V A, which can be qualified as ''bounded,'' the constant initial condition must be smaller than a certain threshold that depends on the value of the delay, as shown in Fig. 2. The coexistence of deterministically bounded and unbounded solutions is of marked importance when the particle is subjected to an additive noise that can drive the particle to large values of x. Indeed, once the particle has reached a large enough value of x, it starts to evolve on a deterministically unbounded trajectory. On this trajectory, the influence of noise on the evolution of the particle is negligible. Thus the probability of escaping from this trajectory is very small. This implies that the quartic potential is in this case metastable, and that a steady-state probability density does not formally exist. However, a pseudo-steady-state probability density can still be defined and used in Eqs. (14) and (17). In addition, as the delay decreases, larger values of x are required in order for the particle to reach a deterministically unbounded trajectory and the average residence time at the bottom of the potential increases. For small values of the delay, the transition between the two wells can therefore be studied without any problem.

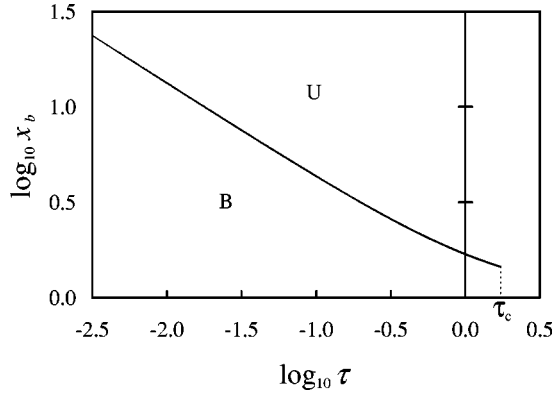

FIG. 2. Boundary x_b between the values of the constant initial condition that lead to a bounded solution (B) of Eq. (26) and those that lead to an unbounded solution (U). For small delays, the position of this boundary seems to approach $x_b \propto 1/\sqrt{\tau}$. For delays larger than $\tau_c \simeq 1.725$, all solutions are unbounded.

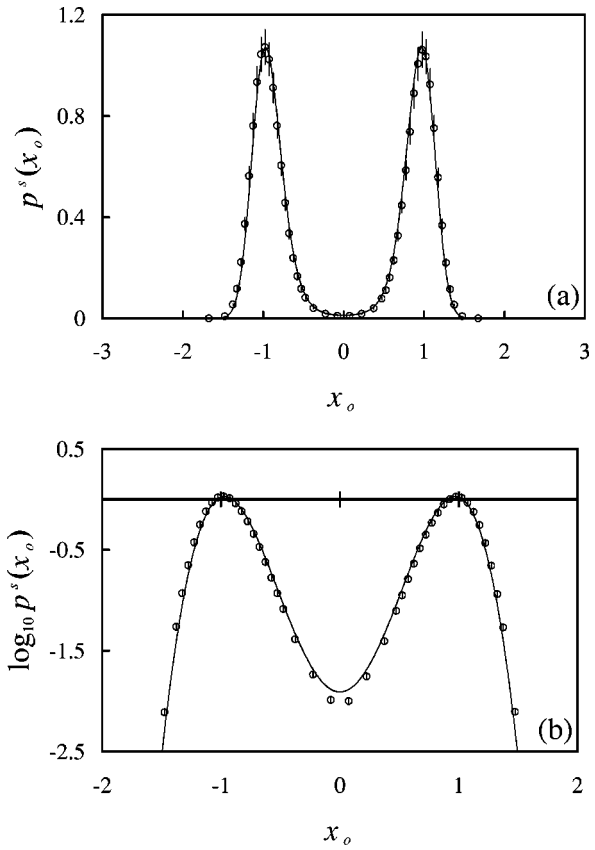

FIG. 3. Steady-state probability density of Eq. (29) for $\tau=\sigma^2=0.1$ on (a) a linear scale and (b) a semilogarithmic scale. The circles represent values obtained by binning sample points from simulations while the solid line comes from Eq. (31). The error bars on the circles are calculated for each bin as the standard deviation of the probability density for a set of simulations.

C. Pseudo-steady-state probability density

When Gaussian white noise is added to Eq. (26), it leads to the SDDE

$$dx(t)=[x(t-\tau)-x^3(t-\tau)]dt+\sigma dW(t). \tag{29}$$

Applying the $O(\tau^2)$ Taylor expansion presented in Sec. IV to Eq. (29) leads to the approximate CAD

$$\overline{f_a^s}(x_o)=\frac{(1-6\tau\sigma^2)x_o-x_o^3}{1-\tau(1-3x_o^2)} \tag{30}$$

and to the approximate pseudo-steady-state probability density

$$p_a^s(x_o)=N_a \exp\left[-\frac{x_o^2}{3\tau\sigma^2}-\frac{1+2\tau-18\tau^2\sigma^2}{9\sigma^2\tau^2}\right.$$
$$\left.\times\ln\left(\frac{1-\tau}{1-\tau+3\tau x_o^2}\right)\right]. \tag{31}$$

Equation (31) is obtained by setting the integration constant c to zero in Eq. (22) and is formally valid for $\tau<1$.

As shown in Fig. 3(a), the pseudo-steady-state probability density is well approximated by Eq. (31) for $\tau=\sigma^2=0.1$.

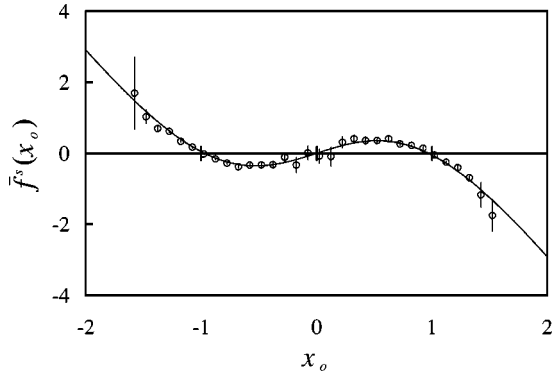

FIG. 4. Steady-state conditional average drift of Eq. (29) for $\tau=\sigma^2=0.1$. The circles represent values obtained from simulations, and the solid line values from Eq. (30). For the simulations, the x_o axis was divided into bins and the quantity $f(x(t-\tau))$ was periodically sampled and binned according to the value of $x(t)$. The steady-state CAD $\overline{f^s}(x_o)$ was then obtained for each bin by calculating the average and the standard deviation of $f(x(t-\tau))$.

Nevertheless, small discrepancies caused by the Taylor expansion can be observed in Fig. 3(b): the two peaks are slightly shifted inwards and the central minimum is shifted upwards. As seen in Sec. V D, these small differences are non-negligible when the pseudo-steady-state probability density is used in Eqs. (14) and (17) to calculate τ_{pop} and $T(x_1,x_2)$. Figure 4 presents the steady-state CAD for these same values of τ and σ^2. For these parameter values, it is well approximated by Eq. (30).

With $\tau=0.1$, $p_a^s(x_o)$ qualitatively agrees with the simulation results as the noise variance is increased up to about $\sigma^2=1$. With $\sigma^2=0.1$, the same is true as the delay is increased up to about $\tau=0.4$. Equation (30) is valid for roughly the same range of parameter values.

Since the mean first passage time [Eq. (17)] and the phenomenological transition rate between the two wells [Eq. (14)] are expressed in terms of the steady-state probability density, using Eq. (31) in conjunction with these two equations leads to valid results when the delay and the noise variance are sufficiently small. For larger delays and noise variances, the steady-state probability density must be determined using numerical simulations.

D. Noise-induced rate processes

As shown in Fig. 5, Eq. (14) leads to values of τ_{pop} that are of the right order of magnitude for a wide range of noise variances and for sufficiently small delays, whether the steady-state probability density in Eq. (14) is determined numerically or using the small delay expansion [Eq. (31)]. However, the ''separation of time scales'' approximation leading to Eq. (14) remains valid for larger delays than the small delay expansion. Indeed, for larger delays, Fig. 5 shows that Eq. (14) better approximates the values of τ_{pop} obtained directly from simulations when the steady-state probability density in that equation is determined from simulations rather than using Eq. (31).

In the case where $\tau=\sigma^2=0.1$, for which the steady-state probability density is presented in Fig. 3, numerical simulations indicated that $\tau_{pop}=341\pm22$, while Eq. (14) used in conjunction with a numerically determined probability density led to $\tau_{pop}=283\pm8$. Even though these two values slightly disagree with one another, they are still reasonably close, and underscore the validity of the separation of time scales approximation for these values of τ and σ^2. For such a small delay, the time scale τ_{int} defined in Sec. III A is expected to be of the same order of magnitude as the time scale over which the univariate probability density $p(x_o,t_o|x',t')$ relaxes within each well. This latter time scale was found to be of order one when $\tau=\sigma^2=0.1$. This was done by numerically calculating the evolution of an initial δ-function probability density centered at $x=-1$, and estimating the relaxation time of its variance within the left well.

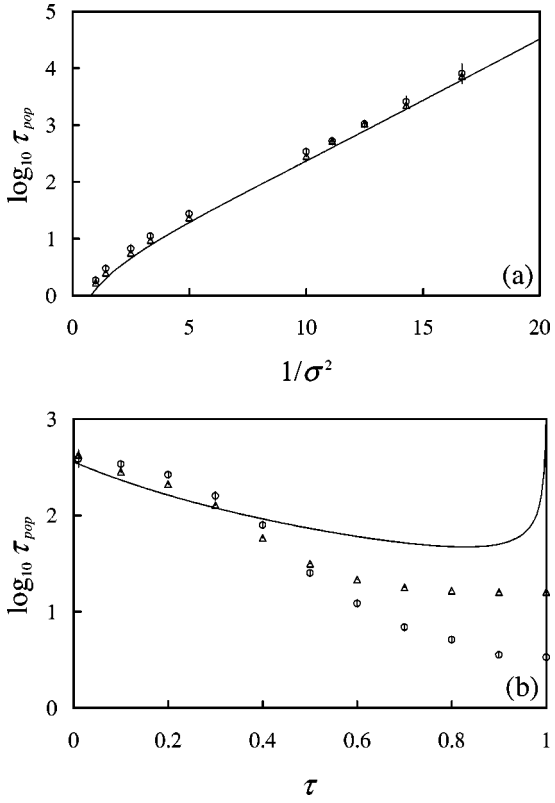

FIG. 5. Time scale τ_{pop} for (a) $\tau=0.1$ and (b) $\sigma^2=0.1$. The circles represent rates obtained directly from sets of simulations where all the realizations are initiated in the left well, and the population number $N_A(t_o|x',t')$ is sampled over time. After initial transients corresponding to relaxation within the left well, $N_A(x_o|x',t')$ decays exponentially over time and is fitted to Eq. (15) in order to obtain τ_{pop} and its standard deviation. The triangles and the solid line both represent values coming from Eqs. (14) and (16), but using two different steady-state probability densities. For the triangles, the steady-state probability density has been determined through repeated simulations, leading to values of τ_{pop} with associated standard deviations. For the solid line, the steady-state probability density has been determined using the small delay expansion [Eq. (31)]. When numerically calculating the pseudo-steady-state probability density from simulations, the particle would sometimes reach an unbounded solution. When this happened, the faulty points were discarded, a new realization was initiated and allowed to relax, and the sampling was resumed using this new realization. In (a), the effective barrier height ΔU appearing in Arrhenius' law has been calculated to be 0.211 ± 0.005 using a linear regression on the six rightmost circles.

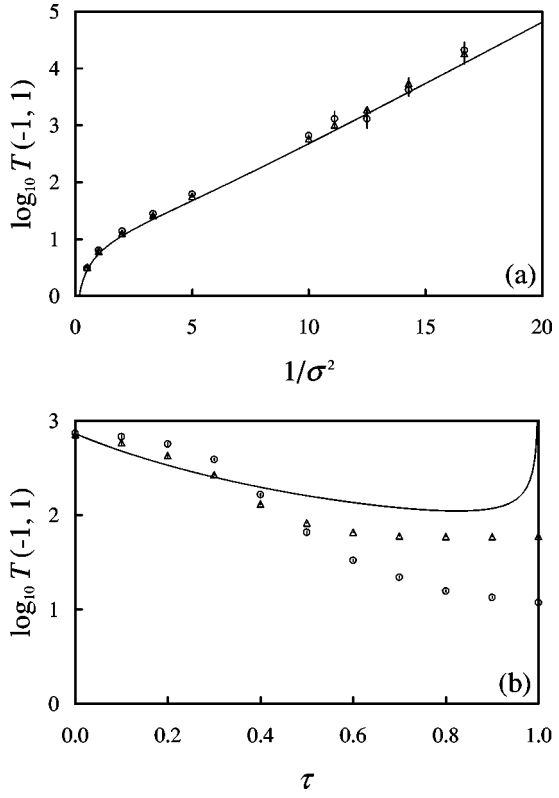

FIG. 6. Mean first passage time $T(x_1,x_2)$ from $x_1=-1$ to $x_2=1$ for (a) $\tau=0.1$ and (b) $\sigma^2=0.1$. The circles are obtained by calculating the mean and the standard deviation of the first passage time for a set of realizations. The triangles and the solid line both represent values coming from Eq. (17a), but using two different steady-state probability densities. For the triangles, the steady-state probability density has been determined from simulations, and for the solid line from the small delay expansion. The error bars on the triangles have been obtained in the same way as in Fig. 5. In (a), the effective barrier height ΔU has been calculated to be 0.21 ± 0.04, using a linear regression on the six rightmost circles.

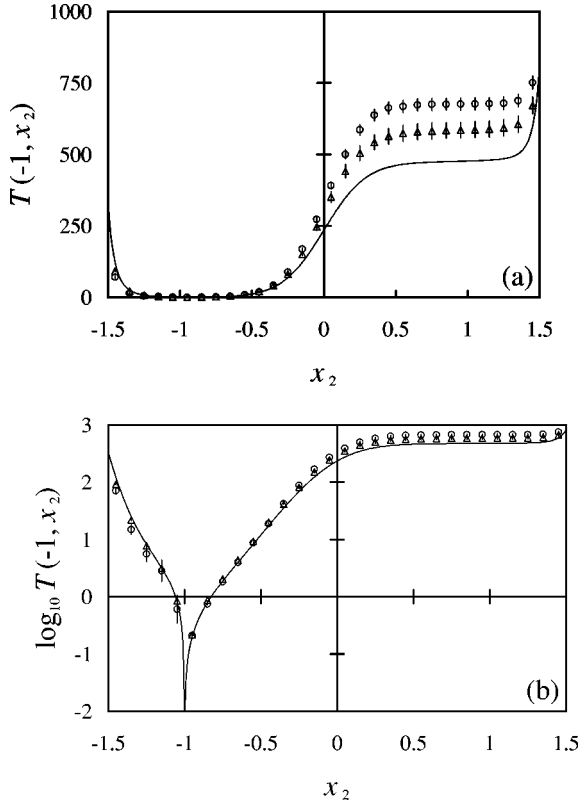

FIG. 7. Mean first passage time $T(x_1,x_2)$ from $x_1=-1$ to several values of x_2 for $\tau=\sigma^2=0.1$ using (a) a linear scale and (b) a semilogarithmic scale. The symbols have the same meaning as in Fig. 6 except that both Eqs. (17a) and (17b) have been used to obtain the triangles and the solid line.

These conclusions about the validity of the separation of time scales assumption and the small delay approximation also apply to the determination of the MFPT using Eqs. (17a) and (17b). In particular, Fig. 6 shows that Eq. (17a) leads to a good approximation of the MFPT $T(-1,1)$ for a large range of noise variances and small delays. Furthermore, Fig. 7 shows that Eqs. (17a) and (17b) adequately approximate $T(-1,x_2)$ on the whole interval $[-1.5,1.5]$ for the case where $\tau=\sigma^2=0.1$. However, the approximation is more accurate for end points x_2 located between the starting point $x_1=-1$ and $x=0$ than for x_2 between 0 and 1.

It is also worth noting from Figs. 5(a) and 6(a) that the logarithms of τ_{pop} and $T(-1,1)$ are inversely proportional to the noise variance when $\tau=0.1$, and the noise variance is small. Thus, for this value of the delay and a small noise variance, both τ_{pop} and $T(-1,1)$ follow Arrhenius' law $e^{\Delta U/\sigma^2}$, where ΔU defines an effective barrier height. As shown in Fig. 8, Arrhenius' law holds even when $\tau=1$, which is significant since the fixed points are not stable for this value of the delay. However, Eqs. (14) and (17) do not accurately predict the effective barrier height ΔU for such a large delay. This discrepancy may arise from the inappropriateness, for values of the delay such that the fixed points are unstable, of projecting the dynamics of the system onto a single degree of freedom. This may also explain why, in Figs 5(a) and 6(a), the difference between the values of τ_{pop} and $T(-1,1)$ obtained from simulations and those obtained using Eqs. (14) and (17) increases with the delay even when $p^s(x_o)$ is determined from simulations. As expected, for a given value of the delay τ, the effective barrier height ΔU is the same for both τ_{pop} and $T(-1,1)$. On the other hand, the effective barrier height is a function of the delay and is different in the $\tau=0.1$ and 1 cases.

VI. DISCUSSION

The Fokker-Planck equation that describes the time evolution of the probability density for a particle evolving in a delayed bistable potential cannot in general be solved exactly. However, the separation of time scales assumption presented in Sec. III leads to a significantly simplifed FPE. This FPE can be used to express the mean time required for the particle to go from one point to another in terms of the noise variance and of the steady-state probability density. This can also be accomplished for the rate coefficients appearing in a phenomenological rate law when the noise variance is small. These quantities can thus be easily determined once the steady-state probability density is known.

As shown in Sec. V with a numerically determined steady-state probability density, these expressions for the mean first passage time and the rate coefficients are in agreement with the results of simulations when there is a good

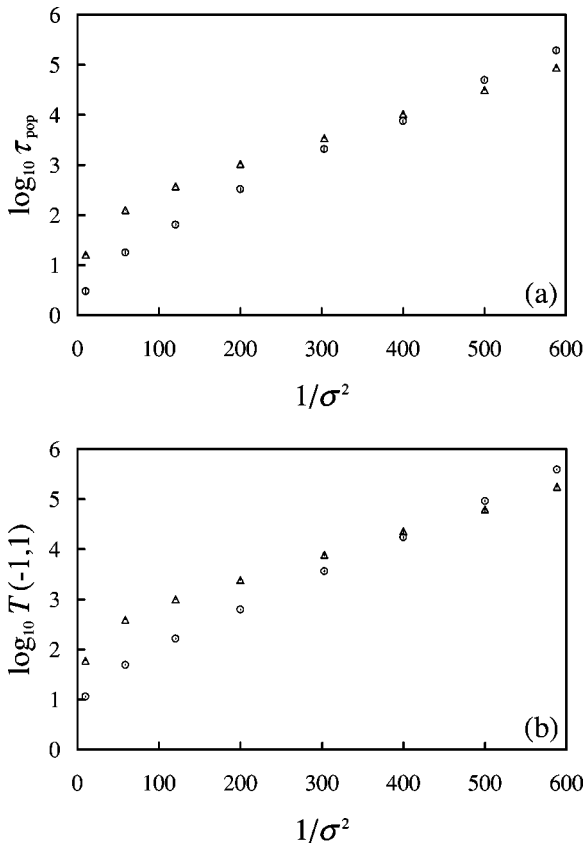

FIG. 8. (a) Time scale τ_{pop} and (b) mean first passage time $T(x_1,x_2)$ from $x_1=-1$ to $x_2=1$ for $\tau=1$. The symbols have the same meaning as in Figs 5 and 6. For the simulation results, the effective barrier height ΔU has been calculated to be $(7.1\pm 0.4)\times 10^{-3}$ in (a) and $(7.19\pm 0.08)\times 10^{-3}$ in (b) using linear regressions on the five rightmost circles. For the points obtained from Eqs. (14) and (17a) in conjunction with a steady-state probability density determined from simulations, ΔU was found to be $(4.94 \pm 0.06)\times 10^{-3}$ in (a) and $(4.77\pm 0.12)\times 10^{-3}$ in (b) using linear regressions on the five rightmost triangles.

separation of time scales. For the case of a particle coupled to a delayed quartic potential, this shows the existence of a region in parameter space where the separation of time scales approximation is valid. Another interesting phenomenon suggested by the simulations is that both the mean first passage time and the phenomenological transition rate follow Arrhenius' law when the noise variance is small, even for large delays.

The small delay expansion [25] summarized in Sec. IV may also be used to determine the steady-state probability density that appears in the formulas obtained using the separation of time scales approximation. For small delays, this approximation leads to values of the mean first passage time and of the phenomenological transition rate that are close to simulation results. However, as the delay increases, the values obtained for these two quantities are more accurate when the steady-state probability density is determined using simulations. Indeed, the small modifications in the steady-state probability density introduced by the Taylor expansion are amplified when calculating the mean first passage time and the phenomenological transition rate. Thus the separation of time scales approximation can be useful for a larger region of parameter space when the steady-state probability density is generated numerically from simulations rather than when using the small delay expansion. Indeed, the Taylor expansion is useful mainly when all the eigenvalues associated with the fixed points are real. When some of the eigenvalues are complex, the approximate system resulting from the Taylor expansion is inappropriate, since it is unidimensional and thus cannot exhibit underdamped oscillations.

A very peculiar property of the deterministic delayed quartic potential that our work has uncovered is the coexistence of bounded and unbounded solutions. As seen in Sec. V B, if a sufficiently large constant initial condition is specified, the particle oscillates around the origin with an ever increasing amplitude. On the other hand, if the constant initial condition is smaller than a threshold that depends on the value of the delay, the trajectory of the particle does not diverge. When subjected to noise, the particle can undergo a transition from a bounded trajectory to an unbounded one. Because of this phenomenon, the details of which are currently being investigated, a steady-state probability density for an overdamped particle in a delayed quartic potential does not formally exist for the type of noise considered here. However, a pseudo-steady-state probability density can still be defined by considering only the dynamics that precedes the transition to unbounded solutions. This pseudo-steady-state probability density can be used to calculate the mean first passage time and the phenomenological transition rate using the formulas presented in this paper.

It would be very interesting to study the influence of the noise correlation time on the phenomenological rate coefficients and on the mean first passage time. The likely appearance of stochastic resonance in this delayed quartic potential, with or without external forcing, could also be investigated. In the presence of external forcing, it may be possible to tune the delay in order to optimize the signal-to-noise ratio. Finally, more theory is needed to understand the origin of Arrhenius' law at large delays, for which the deterministic fixed points are unstable.

ACKNOWLEDGMENTS

The authors are thankful to Frank Moss for discussions during the early stage of this work, to Jacques Laniel for preliminary simulations, and to Robert Maier for his helpful comments. A. L. acknowledges support from the Los Alamos National Laboratory, where work on the delayed quartic potential was initiated. This research was supported by grants from NSERC, IODE, and ONR.

[1] I. L'Heureux and R. Kapral, Phys. Lett. A **136**, 472 (1989).
[2] X.-G. Wu and R. Kapral, J. Chem. Phys. **91**, 5528 (1989).
[3] V. I. Mel'nikov, Phys. Rep. **209**, 1 (1991).
[4] H. A. Kramers, Physica (Amsterdam) **7**, 284 (1940).
[5] P. Hanggi, T. J. Mroczkowski, F. Moss, and P. V. E. McClintock, Phys. Rev. A **32**, 695 (1985).

[6] J. Masoliver, B. J. West, and K. Lindenberg, Phys. Rev. A **35**, 3086 (1987).
[7] I. L'Heureux and R. Kapral, J. Chem. Phys. **88**, 7468 (1988).
[8] I. L'Heureux and R. Kapral, J. Chem. Phys. **90**, 2453 (1989).
[9] I. L'Heureux, R. Kapral, and K. Bar-Eli, J. Chem. Phys. **91**, 4285 (1989).
[10] J. M. Porrà *et al.*, Phys. Rev. A **45**, 6092 (1992).
[11] I. L'Heureux, Phys. Rev. E **51**, 2787 (1995).
[12] S. Guillouzic and I. L'Heureux, Phys. Rev. E **55**, 5060 (1997).
[13] A. Beuter, J. Bélair, and C. Labrie, Bull. Math. Biol. **55**, 525 (1993).
[14] A. Longtin, J. G. Milton, J. E. Bos, and M. C. Mackey, Phys. Rev. A **41**, 6992 (1990).
[15] K. Vasilakos and A. Beuter, J. Theor. Biol. **165**, 389 (1993).
[16] Y. Chen, M. Ding, and J. A. S. Kelso, Phys. Rev. Lett. **79**, 4501 (1997).
[17] J. García-Ojalvo and R. Roy, Phys. Lett. A **224**, 51 (1996).
[18] R. Kapral, E. Celarier, P. Mandel, and P. Nardone, in *Optical Chaos*, Vol. 667 of *Proceedings SPIE (International Society for Optical Engineering)*, edited by N. B. Abraham and J. Chrostowski (SPIE, Bellingham, WA, 1986), pp. 175–182.
[19] H. Grabert and S. Linkwitz, Phys. Rev. A **37**, 963 (1988).
[20] K. Lindenberg, A. H. Romero, and J. M. Sancho, Physica D **133**, 348 (1999).
[21] R. Reigada, A. H. Romero, K. Lindenberg, and J. M. Sancho, J. Chem. Phys. **111**, 676 (1999).
[22] T. Ohira and Y. Sato, Phys. Rev. Lett. **82**, 2811 (1999).
[23] J. Foss, F. Moss, and J. Milton, Phys. Rev. E **55**, 4536 (1997).
[24] S. Kim, S. H. Park, and H.-B. Pyo, Phys. Rev. Lett. **82**, 1620 (1999).
[25] S. Guillouzic, I. L'Heureux, and A. Longtin, Phys. Rev. E **59**, 3970 (1999).
[26] C. W. Gardiner, *Handbook of Stochastic Methods for Physics, Chemistry and the Natural Sciences*, 2nd ed. (Springer-Verlag, New York, 1990).
[27] L. Gammaitoni, P. Hänggi, P. Jung, and F. Marchesoni, Rev. Mod. Phys. **70**, 223 (1998).
[28] W. Gerstner, Phys. Rev. Lett. **76**, 1755 (1996).
[29] S. Kim, S. H. Park, and C. S. Ryu, Phys. Rev. Lett. **79**, 2911 (1997).
[30] M. K. S. Yeung and S. H. Strogatz, Phys. Rev. Lett. **82**, 648 (1999).
[31] P. C. Bressloff and S. Coombes, Physica D **126**, 99 (1999).